Supramolecular Chemistry
Publication details, including instructions for authors and subscription information:
http://www.informaworld.com/smpp/title~content=t713649759

A Study on the Location and Aggregation of Tetrahydrophenylporphyrin with a Single Hexadecyl Chain in Triton X-100 Micelle

Lin Guo[a]; Ying-Qiu Liang[a]
[a] Institute of Mesoscopic Solid State Chemistry and National Key Laboratory of Coordination Chemistry, Nanjing University, Nanjing, P. R. China

To cite this Article Guo, Lin and Liang, Ying-Qiu(2004) 'A Study on the Location and Aggregation of Tetrahydrophenylporphyrin with a Single Hexadecyl Chain in Triton X-100 Micelle', Supramolecular Chemistry, 16: 1, 31 — 40
To link to this Article: DOI: 10.1080/10610270310001592859
URL: http://dx.doi.org/10.1080/10610270310001592859

Supramolecular Chemistry, January–February 2004, Vol. 16 (1), pp. 31–40

Taylor & Francis
Taylor & Francis Group

A Study on the Location and Aggregation of Tetrahydrophenylporphyrin with a Single Hexadecyl Chain in Triton X-100 Micelle

LIN GUO and YING-QIU LIANG*

Institute of Mesoscopic Solid State Chemistry and National Key Laboratory of Coordination Chemistry, Nanjing University, Nanjing 210093, P. R. China

Received (in Austin, USA) 10 July 2002; Accepted 30 May 2003

The location and aggregation of 5,10,15-tris(4-hydroxyphenyl)-20-(hexadecyloxyphenyl)porphyrin (P) in non-ionic polyoxyethylene (9.5) octylphenol (Triton X-100) micelle solutions were studied by means of UV–Vis and fluorescence spectra. P forms premicelle surfactant–porphyrin aggregates when the surfactant concentration is below and approaching the CMC. In Triton X-100 micelle solutions, different types of H-aggregates of P were formed when the concentration of P is higher than 3.9×10^{-6} mol dm^{-3}. As the bulk pH is changed, a transfer process for the porphyrin moiety in Triton X-100 micelle occurs. In neutral Triton X-100 micelle solutions, P may be located at the inner layer of the micelle; in basic conditions, the porphyrin moiety may transfer to the outer surface of the micelle. The kinetic study of porphyrin complexed with Cu(II) in Triton X-100 micelle solutions shows that the metalation rate could be controlled by changing the pH.

Keywords: Porphyrin; Triton X-100; Aggregation; Micelle; Metalation

INTRODUCTION

The porphyrin functional unit located in the photosynthetic reaction center plays an important role in biological processes such as substrate oxidations and conversion of light energy into chemical energy [1–5]. The diverse chemical and photophysical properties of porphyrins are in many cases due to the fact that these molecules are located in very different environments in the membrane matrix. Therefore, special incorporation of porphyrin molecule guests in biomimetic membranes and their functions have been of great interest. Porphyrins anchored to lipid bilayers have successfully been applied to the reversible binding of dioxygen in aqueous solutions [6]. Incorporation of porphyrins in micelles dramatically influences the aggregation mode and location of these molecules and alters their metalation rate [7–9]. It has been suggested that hydrophobic porphyrins can penetrate the lipid regions of membranes and be distributed into the protein-rich membrane domain [10], while highly polar species are supposed to partition mainly in the aqueous compartment [11]. The interaction of water-soluble synthetic porphyrins with ionic micelles has been studied intensively [12,13]. In the presence of ionic surfactants below their critical micelle concentration (CMC), both tetrakis(4-sulfonatophenyl)porphyrin ($TPPS_4$) [14–16] and some *meso*-tetraaryl-substituted picket fence porphyrins [17] were shown to form aggregates. Above CMC, micelles usually solubilize the aggregates of porphyrin derivatives into monomers [12–14,18,19].

So far, however, structural understanding is still unclear, especially for the aggregation and solubilization site of porphyrinic molecules because of their versatile substituents. Although some efforts have been made to study porphyrin aggregation and location in micelle surfactant solutions as well as in aqueous solutions, most of these have concentrated on water-soluble porphyrinic molecules [12–14], and there are still few reports about the amphiphilic porphyrin transfer process in micelles. Moreover, metalation in microheterogeneous media has been less investigated although it is a biological

*Corresponding author. E-mail: linguo@nju.edu.cn (Lin Guo)

ISSN 1061-0278 print/ISSN 1029-0478 online © 2004 Taylor & Francis Ltd
DOI: 10.1080/10610270310001592859

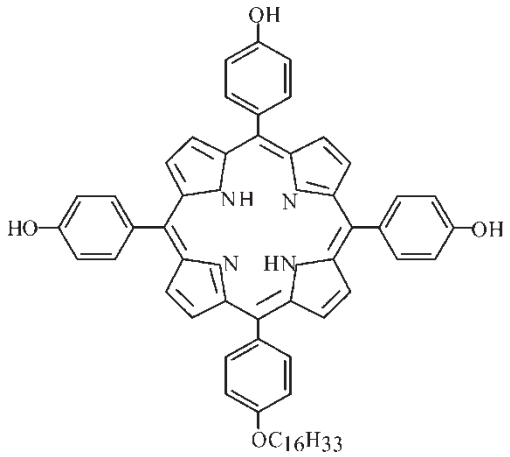

FIGURE 1 Structure of tetrahydrophenylporphyrin with a hexadecyl chain.

phenomenon [9,20]. In this work, an attempt is made to gain more insight into the nature of amphiphilic porphyrin interactions with biological structures using the simplest models for membranes and proteinic reaction centers: aqueous micelles. An amphiphilic porphyrin (**P** shown in Fig. 1) with one hexadecyl chain was solubilized in micelle Triton X-100 solutions. The big porphyrin moieties tend to interact with each other and form aggregates. The co-existence of the hydrophilic hydrophenyl groups and the long hydrophobic chain in the same molecule suggests that such a molecule can be solubilized in organic solvents as well as in the nonpolar region of micelles. Based on this property, the aggregation, location and metalation of **P** in TX-100 micelle will be discussed below.

MATERIALS AND METHODS

Tetrakis(4-hydroxyphenyl)porphyrin (THPP) was prepared first [21], and was then hexadecylated using 1-bromohexadecane in an ethanol solution of potassium hydroxide. The products were then separated and purified four times by thin-layer chromatography over silica gel C with a solvent mixture of chloroform and ethanol as the eluant. 5,10,15-Tris(4-hydroxyphenyl)-20-(4-hexadecyloxyphenyl)porphyrin **P** was obtained and characterized by elemental analysis, MS, IR, and ^{1}H NMR spectroscopy [22,23]. Polyoxyethylene (9.5) octylphenol (Triton X-100) was the analytical reagent. Water was doubly distilled after passing through an ion-exchange resin column. All the organic solvents were analytical grade pure and used without further purification.

Aqueous solutions of **P** in different Triton X-100 concentrations for studying the solubilizing effects of **P** were directly prepared from the solid porphyrin sample. However, in order to make **P** completely soluble, the Triton X-100 micelle, aqueous, organic-water mixture and organic solutions of porphyrin were prepared by injection of a specific amount of a 2.5×10^{-3} mol dm^{-3} dioxane solution of porphyrins into the different solvents to obtain 25 ml solutions. The volume ratio of dioxane and water or other mixture solvents was greater than 1000, so the effects of a trace of dioxane on the solution polarity could be neglected. After 20 min of sonication, the UV–Vis and fluorescence spectra of the solutions were recorded on a Shimadzu UV-3100 spectrophotometer and a Perkin-Elmer LS50B fluorescence spectrophotometer, respectively, using a 1 cm quartz cell. The excitation wavelength (λ_{ex}) was 423 nm. The pH of the solution was measured by a Leici pH-250 pH meter (Shanhai) and the pH was controlled by addition of 1.5 mol dm^{-3} NaOH and 1:4 HCl aqueous solutions. The kinetic processes of the porphyrin complexed with Cu(II) were investigated at room temperature by adding a specific amount of 0.1 mol dm^{-3} $CuSO_4$ aqueous solution to the pH-variable porphyrin-Triton X-100 micelle solutions and then recording the UV–Vis spectra of the mixtures at different reaction times.

RESULTS AND DISCUSSION

Aggregation of P in Triton X-100 Micelle Solution

Figure 2(a) shows the UV–Vis spectra of **P** in different Triton X-100 aqueous solution concentrations. It can be seen that there appears to be no obvious absorption peak within the experimental

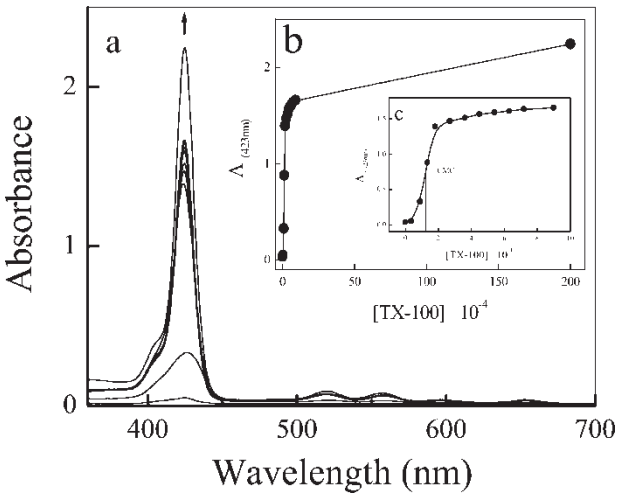

FIGURE 2 (a) UV–Vis spectra of **P** in different Triton X-100 aqueous solution concentrations. (b) Plot of absorbance at 423 nm against the surfactant concentration. (c) Regional plot of b. Concentration of Triton X-100 (mol dm^{-3}): (1) 0; (2) 3.6×10^{-5}; (3) 9.0×10^{-5}; (4) 1.8×10^{-4}; (5) 2.7×10^{-4}; (6) 3.6×10^{-4}; (7) 4.5×10^{-4}; (8) 5.4×10^{-4}; (9) 6.3×10^{-4}; (10) 7.2×10^{-4}; (11) 9.0×10^{-4}.

region in [Triton X-100] = 0 aqueous solutions. This indicates that tetrahydrophenylporphyrin with a single hexadecyl chain has a very low solubility in neutral aqueous solutions. However, as the concentration of Triton X-100 increases, the solubility increases and a characteristic Soret band of **P** appears at 426 nm in 9.0×10^{-5} mol dm^{-3} Triton X-100 solution. As the concentration of Triton X-100 increases up to 1.8×10^{-4} mol dm^{-3}, the Soret band of **P** increases rapidly and the maximum of the Soret band blue shifts to 423 nm. In the case of [Triton X-100] = 9.0×10^{-4} mol dm^{-3}, the absorbance of the Soret band shows some increase while the maximum of the Soret band was not changed. With the concentration of Triton X-100 further increased up to 20×10^{-3} mol dm^{-3}, the absorbance of **P** increases accordingly and the overall absorption characteristics of **P** show no obvious change. It is found that in high surfactant concentration (> CMC) conditions, the absorption characteristics of **P** are similar to those of **P** in an organic solvent in which **P** exists as monomers. These results indicate that **P** can be solubilized as monomers in Triton X-100 micelle solutions. It is clear from Figs. 2(b) and (c) that the absorbance of the Soret band increased abruptly around [Triton X-100] = 1.3×10^{-4} mol dm^{-3}. This value experiences some decrease compared with the CMC of Triton X-100 as reported (3.0×10^{-4} mol dm^{-3}) in the literature [24], indicating that solubilization of the porphyrin molecule in Triton X-100 may reduce the CMC of Triton X-100 micelle.

Another interesting result is that the maximum of the Soret band of **P** is red-shifted from 423 to 426 nm and the full-width at half-height (FWHH) of the Soret band exhibits some broadening with the concentration of surfactants decreasing from 9.0×10^{-4} to 1.8×10^{-4} mol dm^{-3}. These results indicate that the premicelle surfactant–porphyrin aggregates may be formed when the surfactant concentration is below and approaching the CMC. Similar behavior has also been observed in the case of water-soluble porphyrins such as tetrakis(4-sulfonatophenyl)porphyrin interacting with ionic micelles. [7,14]

Figure 3(a) shows the UV–Vis spectra of **P** in TX-100 micelle solution with different porphyrin concentrations. It can be seen from this figure that the Soret bands of **P** appear at 423 nm under low concentration. As the concentration of **P** increased from 2.5×10^{-6} to 9.0×10^{-6} mol dm^{-3}, the overall absorption increased accordingly, and the maximum of the Soret band was blue-shifted from 423 to 421 nm while the full-width at half-height (FWHH) shows some broadening. The blue shift of the Soret band is important evidence for H-type aggregation of porphyrins [14,17]. The plot of absorbance at 423 nm against the concentration, Fig. 3(b), shows

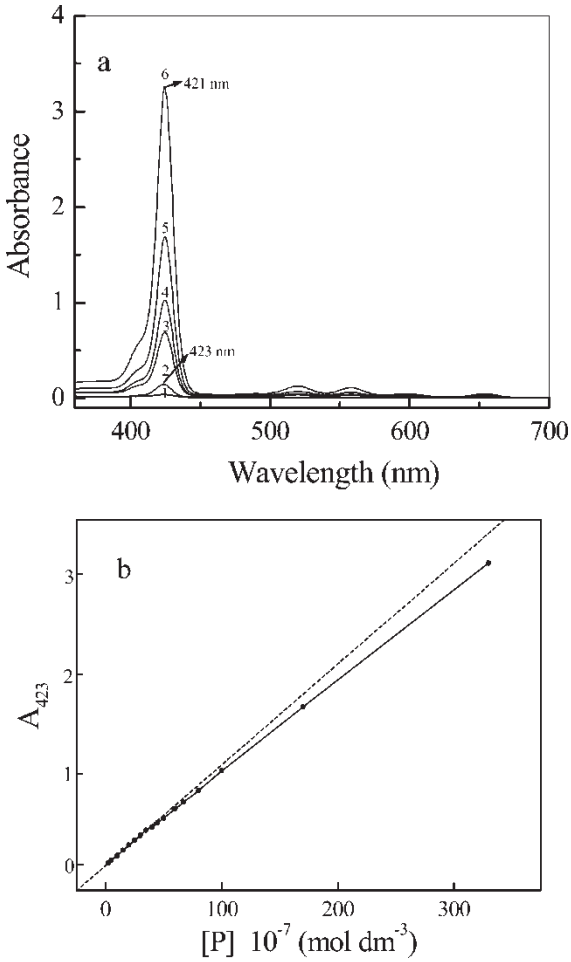

FIGURE 3 (a) UV–Vis spectra of **P** in TX-100 micelle solutions with different porphyrin concentrations (mol dm^{-3}). [**P**]: (1) 2.5×10^{-7}; (2) 1.5×10^{-6}; (3) 6.7×10^{-6}; (4) 1.0×10^{-5}; (5) 1.7×10^{-5}; (6) 3.3×10^{-5}. [Triton X-100] = 9.0×10^{-4}. (b) Plot of absorbance at 423 nm against the concentration of **P**.

that under at low concentration ([**P**] < 3.9×10^{-6} mol dm^{-3}), the plot is linear and follows Beer's law, indicating that **P** exists as monomer (monomer-micelle) under this concentration region with a molar absorbance coefficient (ε) of 1.02×10^{-6} dm/mol cm. However, with the concentration of **P** further increasing, the plot begins to deviate from Beer's law. Deviation of Beer's law is another important proof of porphyrin aggregation [25]. This result indicates that self-aggregates of **P** are formed in TX-100 micelle solutions when the concentration of **P** is higher than 3.9×10^{-6} mol dm^{-3}. Figure (4a) shows the fluorescence emission spectra of **P** in TX-100 micelle solutions at different porphyrin concentrations. The plot of relative intensity at 660 nm against the concentration of **P** is displayed in Fig. 4(b). It can be seen from this figure that under low concentration conditions, the emission band of **P** at 660 nm increases as the concentration of **P** increases. However, when the concentration of **P**

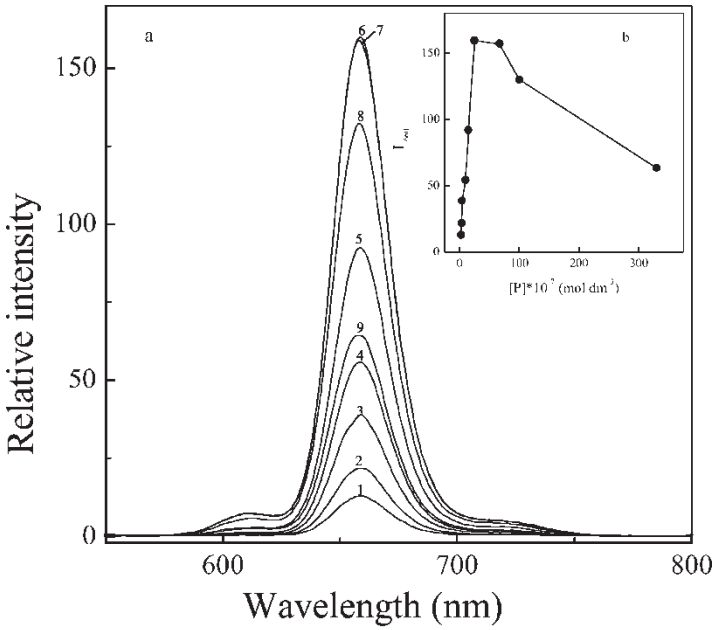

FIGURE 4 (a) Fluorescence emission spectra of **P** in Triton X-100 micelle solutions with different porphyrin concentrations. (b) Plot of relative intensity of 660 nm against the porphyrin concentration (mol dm^{-3}). $\lambda_{ex} = 423$ nm. [**P**]: (1) 2.5×10^{-7}; (2) 1.5×10^{-6}; (3) 6.7×10^{-6}; (4) 1.0×10^{-5}; (5) 1.7×10^{-5}; (6) 3.3×10^{-5}. [Triton X-100] $= 9.0 \times 10^{-4}$ mol dm^{-3}.

increases from 2.5×10^{-6} to 6.7×10^{-6} mol dm^{-3}, the relative intensity of **P** decreases. With the concentration of **P** further increasing, the relative intensity of 660 nm decreases accordingly. It is well accepted that the H-aggregation shows a reduced fluorescence quantum yield [14,26]. Hence, this fluorescence self-quenching behavior of **P** implies H-type aggregation of porphyrin. According to the above results of the UV–Vis and fluorescence spectra (blue shift of the Soret band, widening of FWHH, deviation from Beer's law and reduced fluorescence quantum yield), it can be concluded that different types of H-aggregates of **P** are formed in Triton X-100 micelle solutions when the concentration of **P** is higher than 3.9×10^{-6} mol dm^{-3}.

pH-Controlled Transfer Process of P in Triton X-100 Micelle

It is known that surfactant–dye interaction and dye–dye aggregation are fairly common for oppositely charged dye–detergent pairs and are also possible for neutral dyes [16]. To prevent hydrophobic dyes from undergoing dye–dye aggregation, a low solubilized dye concentration and a relative high surfactant concentration are usually selected. It is known from the above investigations that under conditions of low porphyrin concentration ([**P**] $< 3.9 \times 10^{-6}$ mol dm^{-3}), **P** may exist as monomers in TX-100 micelle solutions. In this paper, a low porphyrin concentration ([**P**] $= 1.0 \times 10^{-6}$ mol dm^{-3}) was used to reduce any disturbance owing to porphyrin aggregation. Moreover, it is known from the above investigation that at 0.9×10^{-3} mol dm^{-3} surfactant concentration solutions, the absorption characteristics of **P** are similar to those of **P** in organic solvent in which **P** exists as monomers. When the concentration of TX-100 was further increased up to 20×10^{-3} mol dm^{-3}, the absorbance of **P** shows some increase and the absorption characteristics of **P** show no obvious change. These phenomena indicate that the concentration of surfactant used in this work (about 3CMC of TX-100) is high enough to prevent porphyrin aggregation. On the other hand, the bulk pH is the only parameter that was changed, hence, the effect of pH on the location and metalation of the porphyrin moiety in the Triton X-100 micelle will be discussed below.

UV–Visible Spectra

Figures 5(a) and (b) show the UV–Vis spectra of the titration of **P** in Triton X-100 micelle solutions. It can be seen that under pH = 6.35 conditions, **P** shows a strong Soret band at 423 nm, and four Q bands appear at 524, 559, 598, 652 nm, respectively. These spectral characteristics are similar to those of the porphyrin monomers in organic solvents (See Table I). When the pH was increased up to 11.05, the Soret band at 423 nm obviously broadens and decreases, the Q bands of **P** shift to 530, 575 and 667 nm, respectively. In the case of pH = 3.51, the overall absorption characteristics are quite similar to those of **P** under pH = 6.35 conditions. This indicates that the porphyrin protonation state is the same at pH 6.35 and 3.51. Figure 5(c) shows the plot of absorbance at 423 nm against the pH. It is clear from this plot that the absorbance at 423 nm decreases

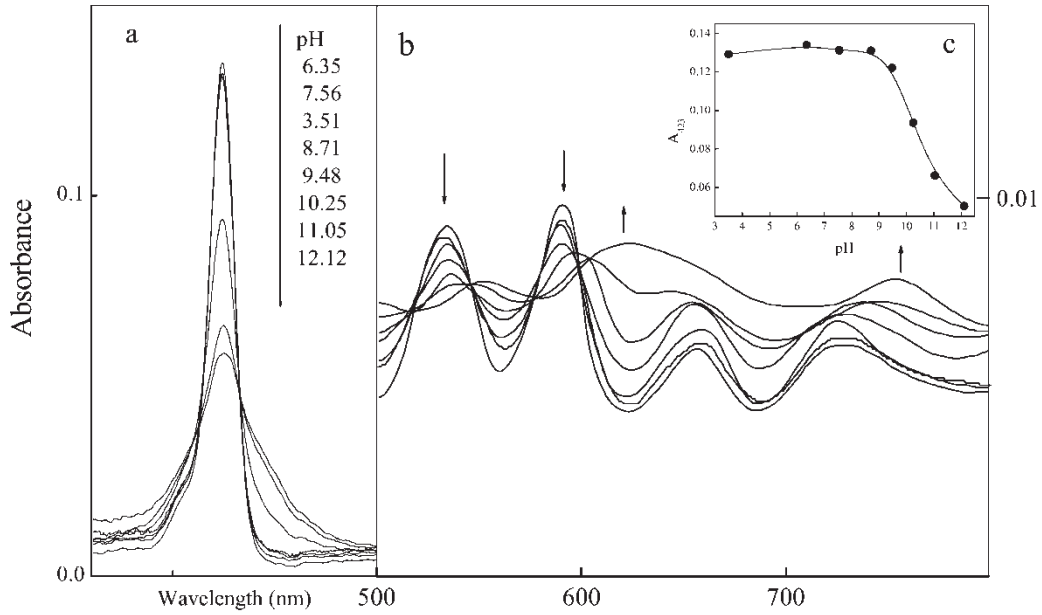

FIGURE 5 (a) UV–Vis spectra [(a) Soret band; (b) Q bands] of **P** in different pH Triton X-100 micelle aqueous solutions. (c) Plot of absorbance of 423 nm against pH. [**P**] $= 1.0 \times 10^{-6}$ mol dm^{-3}; [Triton X-100] $= 9.0 \times 10^{-4}$ mol dm^{-3}.

abruptly when the pH increases up to around 10.5. However, the multi-order deprotonation process of **P** should be considered as well as the large structure of **P**, where three hydroxyphenyl groups should have a different microenvironment, either in the inner part or at the surface of the Triton X-100 micelles; the three hydroxyphenyl groups and the two pyrrole groups of **P** have different dissociations that are each affected by their microenvironment. There must be a complex equilibrium as previously reported [27]. Hence, we were unable to distinguish between the two acid–base equilibria of the porphyrin moiety as well as the p*K* values of the peripheral hydroxys.

It is well known that the absorption Soret bands of porphyrins are often sensitive to the nature of local environments in micelle and aggregation forms [28]. From the analysis of the spectral parameters, such as peak position, intensity, and full-widths at half-height (FWHH) of the Soret band **P** in different solvent environments and in the micelle Triton X-100 solutions, we can draw further conclusions as to what is happening concerning the site solubilization of **P** in Triton X-100 micelles in this pH titration process. It is clear from the data in Table I and Fig. 5 that the absorption spectra characteristics of **P** in micelle Triton X-100 solutions under neutral conditions are very similar to those of monomer **P** in organic solvents rather than those of **P** in aqueous solutions. It can be suggested that the porphyrin moiety of **P** should be located on the inner layer of the Triton X-100 micelle with a weak polarity microenvironment as shown in Fig. 6(a). Such a solubilized location is thermodynamically stable for the hydrophobic hexadecyl chain and the porphyrin moiety even though there are three hydroxyphenyl groups with weak hydrophilic ability. However, the hydrophenyl groups of **P** can be deprotonated consequently to form $\mathbf{P}^{1-}$, $\mathbf{P}^{2-}$ and $\mathbf{P}^{3-}$ ions and the hydrophilic ability of **P** increases in basic solutions. Therefore, the hydrophilic ability of **P** can be adjusted by controlling the pH values. This is a force for the porphyrin macrocycle transferring out of the micelles. In fact, with the bulk pH increasing, a decrease of the Soret band intensity as well as an increase of the FWHH

TABLE I The UV–Vis spectra data of **P** in different solutions*

		Soret band		Q bands (nm)			
Solutions	pH	λ_{max} (nm)	$W_{1/2}$ (nm)	Q_1 (nm)	Q_2 (nm)	Q_3 (nm)	Q_4 (nm)
Triton X-100 micelle	3.51	423	15	524	559	598	652
Triton X-100 micelle	6.35	423	15	524	559	598	652
Triton X-100 micelle	11.05	425	30	530	575	667	
Dioxane	––	421	15	517	556	595	652
Aqueous solution	12.28	435	60	529	577	665	
Aqueous solution	6.20	428	50	525	566	595	655
1.5 M NaOH	Strongly basic	436	65	685	675		

* [**P**] $= 1.0 \times 10^{-6}$ mol dm^{-3}; [Triton X-100] $= 9.0 \times 10^{-4}$ mol dm^{-3}.

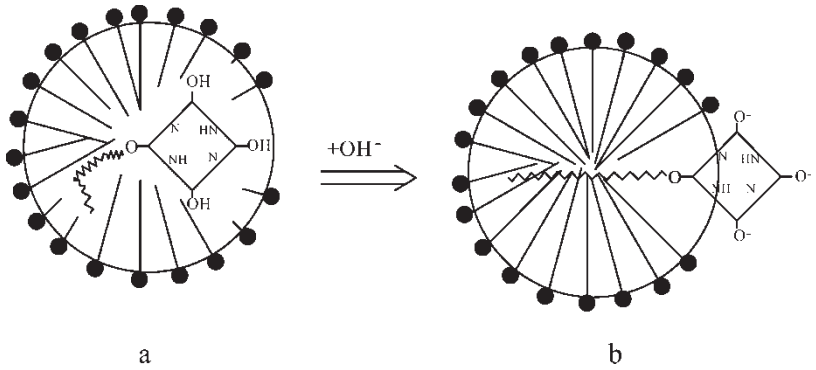

FIGURE 6 Scheme of the transfer process of **P** in Triton X-100 micelle with bulk pH increasing.

were observed, and the overall absorption characteristics of **P** in the pH 11.05 Triton X-100 micelle are quite similar to those of **P** in basic aqueous solutions (Table I). These results infer that **P** may transfer to a strongly polar microenvironment on the outer surface of the Triton X-100 micelle, Fig. 6(b), as the pH increases. Figure 6 shows the scheme of this transfer process.

Another interesting result is the change in the number of Q bands of **P**. Under strongly basic conditions (1.5 M NaOH aqueous solution), the number of Q bands observed changes from four to two (Table I), indicating that the hydrogen atoms that bond to the pyrrole nitrogen atoms of the **P** moiety may also be deprotonated to form a $\mathbf{P}^{5-}$ ion, as deprotonated porphyrin has a higher molecular symmetry (D_{4h}) like metal porphyrins [29]. This deprotonation behavior could also have been observed in cation micelle CTAB solutions, which due to the cation surface potential of the CTAB micelle could provide a strongly basic surface microenvironment under mildly basic conditions [30]. However, the number of Q bands was observed to change from four to three in non-ionic Triton X-100 micelle solutions when the bulk pH increases from 6.35 to 11.05. This behavior indicates that non-ionic micelle Triton X-100 shows no surface potential effects like the cation micelle (CTAB) and the **P** moiety may not be completely deprotonated to form the $\mathbf{P}^{5-}$ ion under this experimental pH condition.

Fluorescence Spectra

It is well accepted that the inner core of a spherical micelle has low polarity and the effective dielectric constants of the Stern layer is around 36 [24]; the outer surface of the micelle as well as the nearby bulk aqueous phase exhibit strong polarity. Therefore, the further from the hydrophobic center of the micelle, the greater the polarity exhibited by the microenvironment. The effect of solvents on the fluorescence spectra of porphyrinic molecules has been studied extensively [31,32]. Figure 7 shows the emission fluorescence spectra of **P** in different solvents. It can be seen from this figure that the fluorescence emission intensity of **P** is sensitive to solvent polarity. In low polarity solvents such as methanol and dioxane, **P** exhibits a very strong emission band at 660 nm and a relatively weak shoulder band at around 610 nm. When the polarity of the solvents increases, the fluorescence intensity of **P** decreases rapidly whereas the fluorescence maximum of **P** at 660 nm is not shifted. **P** shows no obvious emission band within the experimental region in pure aqueous solution. However, the fluorescence emission band at 610 nm is not changed as rapidly as that of the 660 nm band and it even increases in comparison. Based on this behavior, the polar microenvironment of porphyrin in different solvents could be represented by the fluorescence intensity ratio of 610 and 660 nm, $R(I_{610}/I_{660})$. Figure 7(b) shows the plot of the R value of **P** against the dielectric constants of different solvents. It can be seen from this plot that as the dielectric constant of the solvent increases, the intensity ratio of the porphyrin increases proportionately.

Figure 8(a) shows the fluorescence emission spectra of **P** in Triton X-100 micelle solutions at different pH. It is clear from this figure that in weakly acidic solution (pH 3.51 and 6.87), **P** shows a strong emission band at 660 nm and a shoulder band at 610 nm, respectively, similar to that of **P** in an organic solvent with low polarity. With increasing pH, the fluorescence intensity of **P** decreases rapidly. At pH 11.52, the overall fluorescence spectral characteristics of **P** are similar to those of **P** in high polarity aqueous solutions. However, the maximum of the fluorescence band of **P** is not changed. Figure 8(b) displays the plots of relative intensity at 660 nm of **P** against pH in a solution of [Triton X-100] = 9.0×10^{-4} mol dm^{-3} (line 1) and 20×10^{-3} mol dm^{-3} (line 2), respectively. It is clear that the I_{660} intensity abruptly decreases at around pH 10.6 (line 1). This value is similar to that of **P** obtained from UV–Vis spectra. Similar fluorescence quenching behavior could also be observed at 20×10^{-3} mol dm^{-3} (line 2).

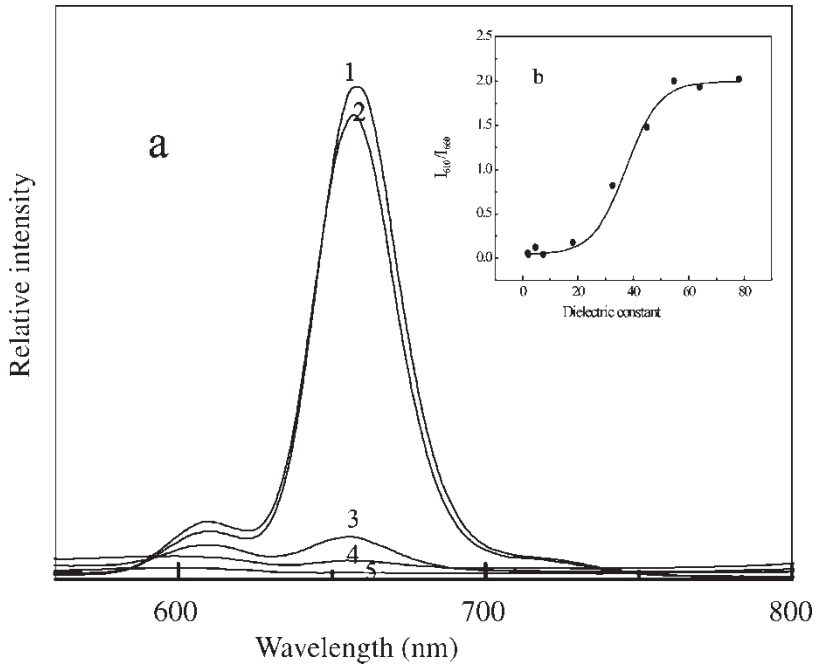

FIGURE 7 (a) Fluorescence spectra of **P** in different solutions. $\lambda_{ex} = 423$ nm; (1) dioxane; (2) 2-propanol; (3) 50% methanol–H_2O; (4) 20% 2-propanol–H_2O; (5) H_2O. (b) Plot of intensity ratios of 610 nm and 660 nm of **P** against the dielectric constants of solvents. The solvents and their dielectric constants used in this experiment from left to right are: dioxane (2.3); chloroform (4.8); tetrahydrofuran (7.6); 2-propanol (18.3); 95% ethanol (26.1); methanol (32.6); 70% MeOH–H_2O (45.0); 50% MeOH–H_2O (54.9); 20% 2-propanol–H_2O (64.1); H_2O (78.5).

A number of factors could influence the relative fluorescence intensity of the porphyrin; one is solvent polarity. The above investigations (Fig. 7) show that increasing the solvent polarity may reduce the quantum yield of fluorescence of **P**; this behavior could also be observed in the case of water-soluble porphyrins [31]. Porphyrin aggregations can also influence the fluorescence relative intensity of the porphyrin. As the dielectric constant (ε) of the solution increases, porphyrins themselves may form different kinds of non-fluorescence aggregates instead of the monomer, which results in the decrease of the fluorescence intensity. In this paper, a low porphyrin concentration was used to decrease any disturbance due to porphyrin aggregation. Consequently, the variation of the fluorescence parameters of porphyrin with pH will now be primarily due to the change in the local microenvironment polarity of **P** in Triton X-100 micelle. Based on the *R* of **P** at different pH values, the corresponding microenvironment polarity of porphyrin in Triton X-100 micelle may be obtained from the information provided by Fig. 7(b). Figure 9 shows the plot of pH against the corresponding microenvironment dielectric constants of **P** in the Triton X-100 micelle. The details of the transfer process of **P** in Triton X-100 micelle was clear from this plot. At pH 6.87, **P** may be located in the inner layer of the Triton X-100 micelle with a microenvironment dielectric constant (ε) around 11. As the pH of the solution increases up to 11.52, the porphyrin moiety transfer to the outer aqueous surface of the Triton X-100 micelle with a strong polar microenvironment ($\varepsilon \approx 46$). These results correspond to the same results obtained by the UV–Vis spectra study. (Fig. 6)

pH-Controlled Metalation Rate of P in Triton X-100 Micelle

It is apparent from the above results that changes in the pH lead to changes in the hydrophilic ability of the porphyrin and eventually to the control of the solubilized location of porphyrin in Triton X-100 micelle. By taking advantage of this property, the metalation of porphyrin in Triton X-100 micelle could also be controlled by changing the pH, which could be shown by the kinetics of the porphyrin complexing with Cu(II).

Figure 10 shows the fluorescence spectra of **P** at pH 9.54 in Triton X-100 micelle solutions before and after complexing with Cu(II). It can be seen from this figure that after 10 h of reaction, the fluorescence intensity of **P** decreases and the fluorescence band at 660 nm almost disappears. This behavior indicates that **P** can complex with Cu(II) and form a non-fluorescent copper complex of **P** under these reaction conditions. Figure 11 shows the UV–Vis spectra of **P** complexed with Cu(II) at different reaction times in a pH 9.54 Triton X-100

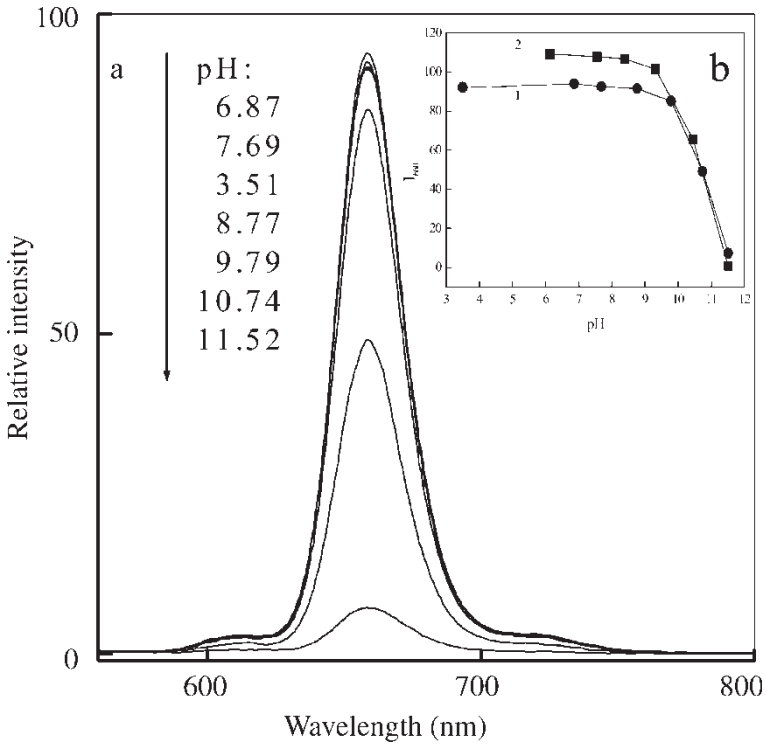

FIGURE 8 (a) Fluorescence spectra of **P** in different pH Triton X-100 micelle solutions. $\lambda_{ex} = 423\,nm$; $[\mathbf{P}] = 2.1 \times 10^{-6}\,mol\,dm^{-3}$; [Triton X-100] $= 9.0 \times 10^{-4}\,mol\,dm^{-3}$. (b) Plot of relative intensity of 660 nm against pH. 1: [Triton X-100] $= 9.0 \times 10^{-4}\,mol\,dm^{-3}$; 2: [Triton X-100] $= 20 \times 10^{-3}\,mol\,dm^{-3}$.

micelle. It can be seen that the four Q bands of **P** decrease with increasing reaction times, while a new band that increases gradually appears at 542 nm. Furthermore, two isosbestic points appear at 530 and 553 nm. This implies that the solubilized location and polar microenvironment of **P** in the Triton X-100 micelle are not changed during metalation in neutral Triton X-100 solution. The kinetic curves of **P** incorporated with Cu(II) are showed in Fig. 11(b); lines 1 and 2 show the decay and increase of the porphyrin absorption at 524 and 542 nm, respectively.

The reaction rate of porphyrin incorporation with Cu(II) could be obtained by detecting the absorbance of porphyrin at different reaction times. As the reaction was performed with a great excess of

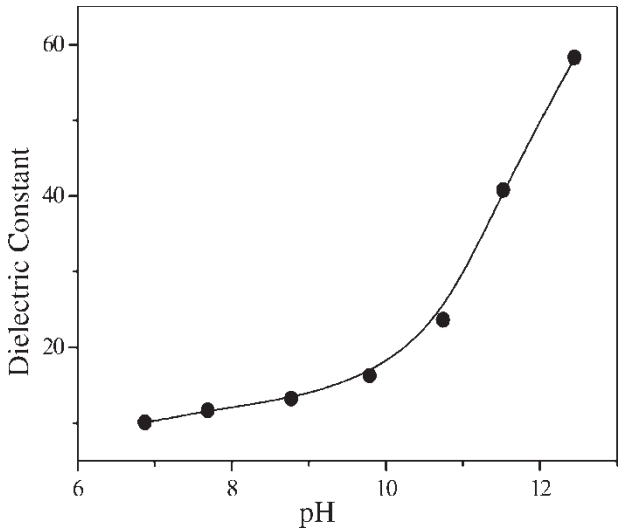

FIGURE 9 Plot of dielectric constants against the pH value of Triton X-100 micelle solutions of **P**.

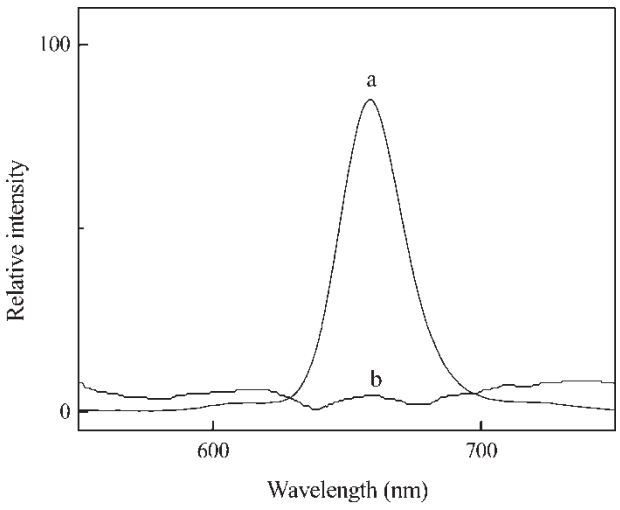

FIGURE 10 Fluorescence spectra of **P** complex with Cu(II) at different reaction times in pH 9.54 Triton X-100 micelle aqueous solution: (a) before adding $CuSO_4$; (b) 10 h after adding $CuSO_4$.

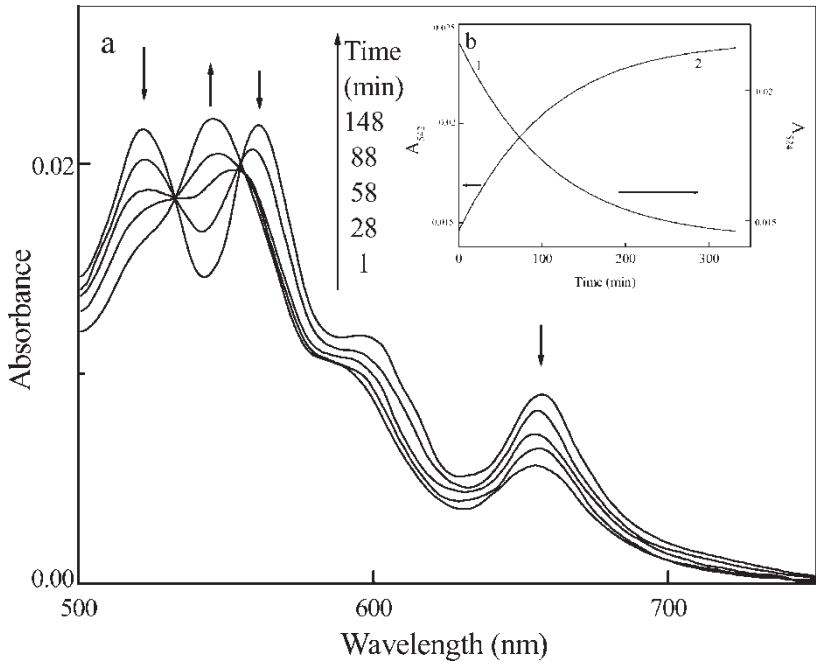

FIGURE 11 (a) UV–Vis spectra of **P** complex with Cu(II) at different reaction times in pH 9.54 Triton X-100 micelle aqueous solution. (b) The kinetic curves of **P** incorporation with Cu(II), lines 1 and 2 show the decay and increase of the porphyrin absorption at 524 nm and 542 nm, respectively. $[Cu^{2+}] = 2.5 \times 10^{-4}$ mol dm^{-3}; [Triton X − 100] $= 9.0 \times 10^{-4}$ mol dm^{-3}.

Cu(II) ([Cu(II)]/[**P**] > 100), the reaction could be regarded as pseudo-first-order reaction [33]. The pseudo-first-order reaction rate constants of the porphyrin complexed with Cu(II) in different pH Triton X-100 micelle solutions (k_ψ) are listed in Table II. It can be seen from this table that as the pH increases from 6.84 to 9.54, the metalation rate constants of **P** increase accordingly.

It is well accepted that Cu(II) is involved in bonding to porphyrin nitrogen atoms and promoted to a plane structure [34]; at the same time it is difficult for the Cu(II) ion to diffuse into the inner nonpolar core of the micelle [9,35]. Hence, the solubilized location of porphyrin in the Triton X-100 micelle greatly influences the metalation rate of porphyrin. If the porphyrin moiety is located at the outer surface of the micelle, the probability of the porphyrin moiety meeting the Cu(II) ion becomes greater, so the metalation rate of porphyrin is greater. When the porphyrin moiety stays at the inner layer of the micelle, although the porphyrin could still form a complex with Cu(II), the metalation rate is relatively low. In this paper, the metalation rates of **P** were measured only in the mildly basic region (pH 6.84–9.54), and a low porphyrin concentration and about 3CMC of Triton X-100 were used to prevent porphyrin aggregation. Hence, the variation of metalation rate of **P** is mainly due to the change of the solubilized location of **P** in Triton X-100 micelles. In the case of neutral Triton X-100 solution, the porphyrin moiety stays at the inner layer of the micelle and the metalation rate is relatively low. As the pH of the solution increases, the porphyrin moiety transfer to the outer layer of the micelle and the probability of the porphyrin encountering Cu(II) ions become higher, hence, the metalation rate of porphyrin increases accordingly.

TABLE II The pseudo-first-order reaction rate constant (k_ψ) of **P*** complexed with Cu(II) in different bulk pH Triton X-100 micelle solutions

pH	k_ψ (min^{-1})
6.84	2.5×10^{-3}
7.59	3.1×10^{-3}
8.56	5.3×10^{-3}
9.54	9.2×10^{-3}

* [**P**] $= 2.1 \times 10^{-6}$ mol dm^{-3}; $[Cu^{2+}] = 2.5 \times 10^{-4}$ mol dm^{-3}; [Triton X-100] $= 9.0 \times 10^{-4}$ mol dm^{-3}.

CONCLUSIONS

A UV–Vis and fluorescence spectra study of the synthesized amphiphilic 5,10,15-tris(4-hydroxyphenyl)-20-(hexadecyloxyphenyl)porphyrin **P** in non-ionic polyoxyethylene (9.5) octylphenol (Triton X-100) micelle solutions and different solvents shows that **P** forms premicelle surfactant–porphyrin aggregates when the surfactant concentration is below and approaching the CMC and different kinds of H-aggregates in Triton X-100 micelle solutions when the concentration of **P** is higher than 3.9×10^{-6} mol dm^{-3}. As the pH is changed a transfer

process for the porphyrin moiety in the Triton X-100 micelle occurs. In neutral Triton X-100 micelle, **P** may be located at the inner layer of the micelle. The porphyrin moiety transfers to the outer surface of the Triton X-100 micelle under basic conditions. The kinetic study of porphyrin complexing with Cu(II) shows that the metalation rate of porphyrin increases as the pH increases, indicating that metalation rate could be controlled by changing the pH.

Acknowledgements

This work was financially supported by the Natural Science Foundation of China with a grant (No. 20073019).

References

[1] Miyasaka, T.; Watanabe, T.; Fujishima, A.; Honda, K. *J. Am. Chem. Soc.* **1978**, *100*, 6657.
[2] Miyasaka, T.; Watanabe, T.; Fujishima, A.; Honda, K. *Nature* **1979**, *277*, 638.
[3] Drain, C. M.; Gentemann, S.; Roberts, J. A.; Helson, N. Y.; Medforth, C. J.; Jia, S. L.; Simpson, M. C.; Smith, K. M.; Fajer, J.; Shelnutt, J. A.; Holten, D. *J. Am. Chem. Soc.* **1998**, *120*, 3781.
[4] Steinberg-Yfrach, G.; Liddell, P. A.; Hung, S.-C.; Moore, A. L.; Gust, D.; Moore, T. A. *Nature* **1997**, *385*, 239.
[5] Kano, K.; Migake, T.; Uomoto, K.; Sato, T.; Ogawa, T.; Hashimoto, S. *Chem. Lett.* **1983**, *144*, 1867.
[6] Tsuchida, E.; Nishide, H. *Top. Curr. Chem.* **1986**, *132*, 63.
[7] Gandini, S. C. M.; Yushmanov, V. E.; Borissevitch, I. E.; Tabak, M. *Langmuir* **1999**, *15*, 6233.
[8] Barber, D. C.; Whiten, D. G. *J. Am. Chem. Soc.* **1987**, *109*, 6842.
[9] Rao, V. H.; Krishhan, V. *Inorg. Chem.* **1985**, *24*, 3538.
[10] Ricchelli, F.; Gobbo, S.; Jori, G.; Moreno, G.; Vinzens, F.; Salet, C. *Photochem. Photobiol.* **1993**, *58*, 53.
[11] Ricchelli, F.; Jori, G. *Photochem. Photobiol.* **1986**, *44*, 151.
[12] Kadish, K. M.; Maiya, G. B.; Araullo, C.; Guilard, R. *Inorg. Chem.* **1989**, *28*, 2725.
[13] Kadish, K. M.; Maiya, G. B.; Araullo, C. *J. Phys. Chem.* **1991**, *95*, 427.
[14] Maiti, N. C.; Mazumdar, S.; Periasamy, N. *J. Phys. Chem. B* **1998**, *102*, 1528.
[15] Tominaga, T.; Endoh, S.; Ishimaru, H. *Bull. Chem. Soc. Jpn.* **1991**, *64*, 942.
[16] Schmehl, R. H.; Whitten, D. G. *J. Phys. Chem.* **1981**, *85*, 3473.
[17] Barber, D. C.; Freitag-Beeston, R. A.; Whitten, D. G. *J. Phys. Chem.* **1991**, *95*, 4074.
[18] Mazumdar, S.; Medhi, O. K.; Mitra, S. *Inorg. Chem.* **1988**, *27*, 2541.
[19] Simplicio, J. *Biochemisry* **1972**, *11*, 2525.
[20] Lavallee, D. K. *Coord. Chem. Rev.* **1985**, *61*, 55.
[21] Little, R. G. *J. Heterocycl. Chem.* **1981**, *18*, 129.
[22] Tian, Y. C.; Wang, Y. Q.; Huang, T.; Liang, Y. Q. *Bull. Inst. Chem. Rev. Kyoto Univ.* **1993**, *71*, 86.
[23] Wang, Y. Q. Ph. D. Dissertation, Jilin University, Changchun, 1993.
[24] Fendler, J. H. *Membrane Mimetic Chemistry*; John Wiley and Sons, 1982; Chapter 2.
[25] Pasternack, R. F.; Huber, P. R.; Boyd, P. *J. Am. Chem. Soc.* **1972**, *94*, 4511.
[26] Van Esch, J. H.; Feiters, M. C.; Peters, A. M.; Nolte, R. J. M. *J. Phys. Chem.* **1994**, *98*, 5541.
[27] Kanno, K.; Minamizono, H.; Kitae, T.; Negi, S. *J. Phys. Chem. A* **1997**, *101*, 6118.
[28] Vermathen, M.; Louie, E. A.; Chodosh, A. B.; Sandra Reid, C.; Simonis, U. *Langmuir* **2000**, *16*, 210.
[29] Gouterman, M. *J. Mol. Spectrosc.* **1961**, *6*, 138.
[30] Zhang, Y. H.; Guo, L.; Li, Q. S.; Wang, Y. Q. *Chem. J. Chin. Univer.* **1997**, *18*, 1703.
[31] Pan, Z.; Xu, M.; Li, J. *J. WuHan Univers. Nature Sci. Ed.* **1993**, *4*, 51.
[32] Chirrony, V. S.; Hoek, A. V.; Schaafsma, T. J.; Pershukerich, P. P.; Filatov, I. V.; Avilov, I. V.; Shishporenok, S. I.; Terekhov, S. N.; Malinovskii, V. L. *J. Phys. Chem. B* **1998**, *102*, 9714.
[33] Jin, S. *Theory of Liquid State Chemical Reaction Kinetic*; Shanghai Tech.: Shanghai, 1984.
[34] Falk, J. E. *Porphyrins and Metal Porphyrins*; Smith, K. M., Ed.; Elsevier: New York, 1975.
[35] Williams, G. M.; Willams, R. F. X.; Lewis, A. *J. Inorg. Nucl. Chem.* **1979**, *41*, 441.